J|A|C|S ARTICLES

Published on Web 05/28/2009

A Multiscale Scheme for the Simulation of Conformational and Solution Properties of Different Dendrimer Molecules

Gustavo Del Río Echenique,[†] Ricardo Rodríguez Schmidt,[†] Juan J. Freire,[‡] José G. Hernández Cifre,[†] and José García de la Torre*,[†]

Departamento de Química Física, Facultad de Química, Universidad de Murcia, 30071 Murcia, Spain, and Departamento de Ciencias y Técnicas Fisicoquímicas, Facultad de Ciencias, Universidad Nacional de Educación a Distancia, 28040 Madrid, Spain

Received February 18, 2009; E-mail: jgt@um.es

Abstract: We propose a multiscale protocol for the simulation of conformation and dynamics of dendrimer molecules in dilute solution. Conformational properties (radius of gyration, mass distribution, and scattering intensities) and overall hydrodynamic properties (translational diffusion and intrinsic viscosity) are predicted by means of a very simple coarse-grained bead-and-spring model, whose parameters are not adjusted against experimental properties, but rather they are obtained from previous, atomic-level simulations which are also quite simple, performed with small fragments and Langevin dynamics simulation. The scheme is described and applied systematically to four different dendrimer molecules with up to seven generations. The predictive capability of this scheme is tested by comparison with experimental data. It is found that the predicted geometric and hydrodynamic radii of the dendrimer molecules are in agreement (typical error is about 4%) with a large set experimental values of the four dendrimers with various numbers of generations. Agreement with some X-ray scattering experimental intensities also confirms the good prediction of the internal structure. This scheme is easily extendable to study more complex molecules (e.g., functionalized dendrimers) and to simulate internal dynamics.

1. Introduction

In scarcely two decades after the seminal papers by Tomalia et al.,[1−3] dendritic molecules have evolved from a fascinating and promising but extremely difficult topic to accessible and remarkably useful chemical entities.[4,5] The extraordinary range of applications of these molecules, from catalysis to drug delivery, has motivated a large body of research on dendrimers. From the point of view of polymer physical chemistry, their hyperbranched but regular structure and some peculiarities in their dilute solution properties motivated original—and in some cases controversial—descriptions of the structure−properties relationships of dendrimers.[6,7] Such relationships are not mere academic problems but present a really practical importance, as they determine—in addition to their conventional solution properties—the performance of these molecules in a variety of applications.

As a consequence of their hyperbranched and regular architecture, dendrimers may appear as globular nanoparticles; however, they are not very densely packed, and indeed their density is not uniform. Furthermore, while their overall shape may seem nearly spherical, they are not rigid but instead exhibit a rich internal dynamics. These aspects, which are crucial for both conventional properties and practical applications, are difficult to deal with just theoretical descriptions, and therefore (as it happened with their cousin molecules, globular proteins) computer simulation has become an essential tool for their study. A straightforward approach is the molecular dynamics simulation of dendrimer molecules with atomic detail, facilitated by the availability of software packages that implement this technique.[8−11] The well-known drawback of this approach is that it may not reach the range of times that are characteristic in some of the functions of dendrimers. On the other hand, simulations for coarse-grained models of dendrimers, inspired in the classical bead-and-connector models used in polymer physics,[12−19] do provide insight on essential features of the conformation and dynamics of dendrimers but may lack the

[†] Universidad de Murcia.
[‡] Universidad Nacional de Educación a Distancia.

(1) Tomalia, D. A.; Baker, H.; Dewald, J. R.; Hall, M. R.; Kallos, G.; Martin, S. J.; Roeck, J.; Ryder, J.; Smith, P. B. *Polym. J.* **1985**, *17*, 117.
(2) Tomalia, D. A.; Naylor, A. M.; Goddard, W. A., III. *Angew. Chem., Int. Ed. Engl.* **1990**, *29*, 138.
(3) Tomalia, D. A.; Hedstrand, D. M.; Ferritto, M. S. *Macromolecules* **1991**, *24*, 1435.
(4) *Dendrimers and Other Dendritic Polymers*; Fréchet, J. M., Tomalia, D. A., Eds.; Wiley: New York, 2001.
(5) Halford, B. *Chem. Eng. News* **2005**, *83*, 30.
(6) de Gennes, P. G.; Hervet, H. *J. Phys., Lett.* **1983**, *44*, 351.
(7) Lescanec, R. L.; Muthukumar, M. *Macromolecules* **1990**, *23*, 2280.
(8) Gorman, C. B.; Smith, J. C. *Polymer* **2000**, *41*, 675.
(9) Lee, I.; Athey, B. D.; Wetzel, A. W.; Meixner, W.; Baker, J. R., Jr. *Macromolecules* **2002**, *35*, 4510.
(10) Han, M.; Chen, P.; Yang, X. *Polymer* **2005**, *46*, 3481.
(11) Lee, H.; Larson, R. G. *J. Phys. Chem. B* **2006**, *110*, 4014.
(12) Mansfield, M. L.; Klushin, L. I. *Macromolecules* **1993**, *26*, 4262.
(13) Murat, M.; Grest, G. S. *Macromolecules* **1996**, *29*, 1278.
(14) Carl, W. *Macromol. Theory Simul.* **1996**, *5*, 1.
(15) Yu Chen, Z.; Cui, S.-M. *Macromolecules* **1996**, *29*, 7943.
(16) Lyulin, A. V.; Davies, G. R.; Adolf, D. B. *Macromolecules* **2000**, *33*, 3294.
(17) Mansfield, M. L. *Macromolecules* **2000**, *33*, 8043.
(18) Lyulin, S. V.; Darinskii, A. A.; Lyulin, A. V. *Macromolecules* **2005**, *38*, 3990.
(19) Bosko, J. T.; Prakash, J. R. *J. Chem. Phys.* **2008**, *128*, 034902.

 10.1021/ja901275d CCC: $40.75

detail needed to make precise, quantitative predictions of properties of specific molecules. An illuminating and comprehensive review of the whole field of computer simulation of dendrimers has been published by Ballauff and Likos.[20]

Coarse-grained models may predict properties of individual molecules by an appropriate choice of adjustable parameters. As shown in previous works,[21−25] atomistic simulations may help to assign some parameters of such models, while others parameters had to be adjusted as to fit some pieces of experimental information and then used to predict other properties.

In the present work we have intended to develop a protocol to predict solution properties of dendrimers in a multiscale approach. The prediction is made with a very simple coarse-grained model. However, none of the parameters of such a model is adjustable; instead all are taken from atomistic simulations, which are not performed on the whole dendrimer but on small molecular pieces (branches, "Y" junctions, etc.), carrying such atomistic simulations in very simple ways, like Langevin dynamics. This kind of multiscale approach is being frequently used in the simulation of properties of biological macromolecules.[26] In our work, for the atomistic calculation of the effective radius of the units (branches) we employ bead modeling techniques, implemented in public-domain tools that have been shown to be extremely useful for biomolecules,[27] and we also use other public-domain programs for the simulation of the coarse-grained model.[28,29] Thus, the present work proposes a unified protocol—in regard to both model and simulation methodology—which is applied in the same way to four dendrimers: monodendrons and tridendrons of polybenzylether (mono-PBzE, tri-PBzE),[30,31] polyamidoamine (PAMAM),[1,32] and polypropylenimine (PPI).[33] The chemical structures of the core and the branches of these dendrimers are displayed in Figure 1. The cores are based on 3,5-dihydroxybenzyl alcohol for mono-PBzE, 1,1,1-tris(4′-hydroxyphenyl)ethane for tri-PBzE, ethylenediamine (EDA) for PAMAM, and 1,4-diaminobutane (DAB) for PPI.

We have tried to be quite comprehensive not only including in our study the four dendrimers which have been sufficiently characterized in solution but also considering the various properties that are experimentally available, both hydrodynamic—particularly the intrinsic viscosity $[\eta]$—and conformational, like the radius of gyration R_g obtained from X-ray scattering, and the angular dependence of scattering intensities. We also predict other hydrodynamic and conformational properties, like translational diffusion coefficient, and distributions of mass and distances, that describe further aspects of the internal structure and behavior of dendrimers in solution. For the sake of brevity, we present in the main body of this paper a selection of examples and results for some properties and some molecules, along with summarizing conclusions which demonstrate how the predictions agree with experimental data. In the Supporting Information, an Appendix gives full details for all the cases.

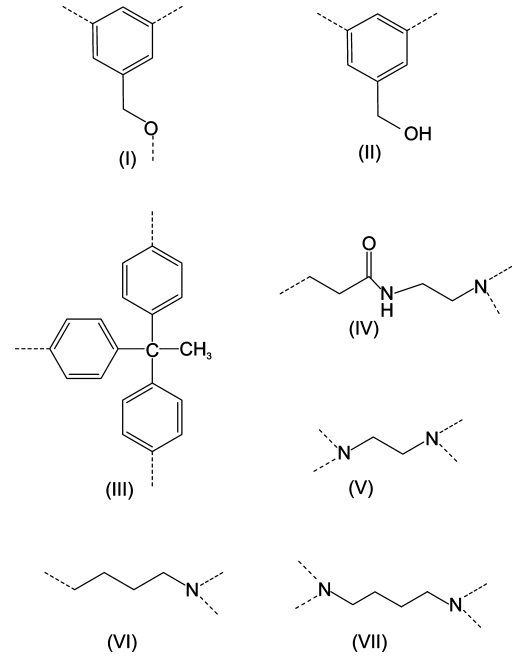

Figure 1. Chemical structures (I) PBzE branch; (II) mono-PBzE core; (III) tri-PBzE core; (IV) PAMAM-EDA branch; (V) PAMAM-EDA core; (VI) PPI-DAB branch; (VII) PPI-DAB core.

2. Models and Simulation Protocol

2.1. Mesoscale Model. The model that will be ultimately used for the prediction of the conformation and properties in solution is a coarse-grained, beads-and-springs model, having one bead per branch or repeating unit, thus providing an adequate, mesoscale representation of architecture of the dendrimer molecule. A scheme of the model, corresponding to a mono-PBzE with three generations is presented in Figure 2. The model has N beads, one representing the core and the remaining $N - 1$ are the branches. Each bead is attached to a previous one by one connector, so that the model contains $N - 1$ linear springs to represent this connectivity.

We must remark that according to the criterion used in this work, also followed by some authors,[1,21] the first generation of a dendrimer ($G = 1$) comprises the branches emerging directly from the core. However, other authors consider that primary structure (our $G = 1$) as generation zero ($G = 0$),[34,35] and therefore their generation $G = 1$ corresponds to our generation $G = 2$, and so on.

For the linear springs linking neighboring beads we have devised in this work a potential that is a hybrid of Fraenkel

(20) Ballauff, M.; Likos, C. N. *Angew. Chem., Int. Ed.* **2004**, *43*, 2998.
(21) Freire, J. J.; Rodríguez, E.; Rubio, A. M. *J. Chem. Phys.* **2005**, *123*, 1549901–1.
(22) Del Río Echenique, G.; Hernández Cifre, J. G.; Rodríguez, E.; Rubio, A.; Freire, J. J.; García de la Torre, J. *Macromol. Chem. Macromol. Symp.* **2007**, *245*, 386.
(23) Rodríguez, E.; Freire, J. J.; Del Río Echenique, G.; Hernández Cifre, J. G.; García de la Torre, J. *Polymer* **2007**, *48*, 1155.
(24) Freire, J. J.; Rubio, A. M. *Polymer* **2008**, *49*, 2762.
(25) Freire, J. J. *Soft Matter* **2008**, *4*, 2139.
(26) Ayton, G. S.; Noid, W. G.; Voth, G. A. *Curr. Opin. Struct. Biol.* **2007**, *17*, 192.
(27) García de la Torre, J.; Huertas, M. L.; Carrasco, B. *Biophys. J.* **2000**, *78*, 719.
(28) García de la Torre, J.; Pérez Sánchez, H. E.; Ortega, A.; Hernández Cifre, J. G.; Fernandes, M. X.; Díaz Banos, F. G.; López Martínez, M. C. *Eur. Biophys. J.* **2003**, *32*, 477.
(29) García de la Torre, J.; Ortega, A.; Pérez Sánchez, H. E.; Hernández Cifre, J. G. *Biophys. Chem.* **2005**, *116*, 121.
(30) Hawker, C. J.; Fréchet, J. M. J. *J. Am. Chem. Soc.* **1990**, *112*, 7638.
(31) Mourey, T. H.; Turner, S. R.; Rubinstein, M.; Fréchet, J. M. J.; Hawker, C. J.; Wooley, K. L. *Macromolecules* **1992**, *25*, 2401.
(32) Uppuluri, S.; Keinath, E. S.; Tomalia, D. A.; Dvornic, P. R. *Macromolecules* **1998**, *31*, 4498.
(33) de Brabander-van den Berg, E. M. M.; Meijer, E. W. *Angew. Chem., Int. Ed. Engl.* **1993**, *32*, 1308.
(34) Karatasos, K.; Adolf, D. B.; Davies, G. R. *J. Chem. Phys.* **2001**, *115*, 5310.
(35) Prosa, T. J.; Bauer, B. J.; Amis, E. J. *Macromolecules* **2001**, *34*, 4897.

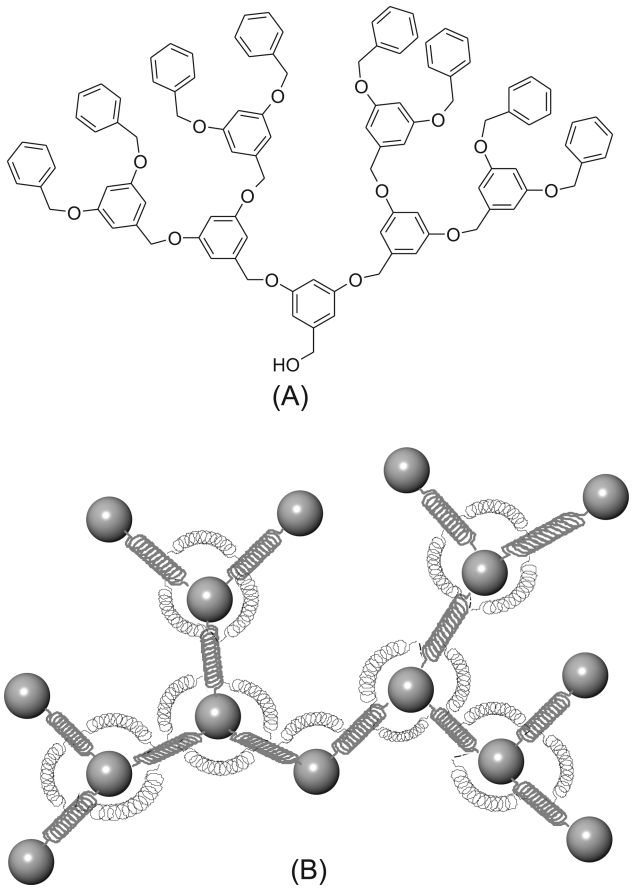

Figure 2. Scheme of dendrimer model: (A) chemical structure of a mono-PBzE molecule with $G = 3$; (B) its coarse-grained bead-and-spring model.

(hard Hookean) and FENE (finitely extensible, nonlinear elastic) springs.[36] As an elastic connector representing a chemical entity, the spring must have an equilibrium length l_e and a Hookean spring constant H_{HF} that gauges the fluctuation of the instantaneous length l. Also, to account for the limited extensibility of the dendrimer branches, the potential includes a maximum length, l_{max}, and all these features of our "hard-FENE" springs are represented by the equation

$$V_{conn}(l) = -\frac{1}{2}H_{HF}l_{\max}^2 \ln\left(1 - \frac{l^2}{l_{\max}^2}\right) - \frac{1}{2}H_{HF}l_{\max}l_e \ln\left(\frac{l_{\max} + l}{l_{\max} - l}\right) \quad (1)$$

Figure S1A in the Supporting Information illustrates the form of the potential defined by eq 1 for the case of mono-PBzE and compares it to other commonly employed spring potentials.

The disposition of the "child" branches with respect to their "mother" is limited by the restricted conformational freedom at the branching points. In our model, this is represented by angular springs, for which we adopt a simple quadratic potential,

$$V_{ang}(\alpha) = \frac{1}{2}Q(\alpha - \alpha_0)^2 \quad (2)$$

where α is the supplementary angle to the bond angle ($\alpha = 0$ for aligned connectors), α_0 is the equilibrium angle, and Q is the bending constant.

We must also include excluded volume (EV) interactions between nonbonded beads. For the sake of simplicity that inspires our model, the EV effect is represented by a purely repulsive hard sphere (HS) potential: if the distance between two nonbonded beads is less or equal than the contact distance, σ_{HS}, the potential value becomes infinity (in practice a sufficiently high value), and otherwise the potential value is zero. The calculation of hydrodynamic properties requires the assignment of a hydrodynamic (Stokes) radius to the beads, a. Again, with the intention of maximum simplicity we have decided that this radius would also be the hard-sphere radius for the EV effect, so that $\sigma_{HS} = 2a$ (or the sum of the values of a radius for a branch and the core). Thus, the set of values of a, l_e, H_{HF}, l_{max}, Q, and α_0 defines completely the mechanical (conformational and dynamic) behavior of our mesoscale model of the dendrimer.

2.2. Monte Carlo Simulation and Hydrodynamics. The prediction of properties for our partially flexible dendrimer models is done by using an importance sampling Monte Carlo procedure. In addition to conformational properties, like the root-mean-square radius of gyration, R_g, and various distance distributions, we compute hydrodynamic properties by using the rigid-body Monte Carlo (RBMC) method.[37−39] In the RBMC procedure, the properties are evaluated as means of the calculated values for each conformation in the Monte Carlo sample, as if the conformation were an instantaneously rigid particle. We have recently presented a public-domain program, MONTEHYDRO[29] (available from http://leonardo.inf.um.es/macromol), which carries out both the Monte Carlo generation of conformations and the calculation of individual and average values for a general bead-and-connector model of arbitrary topology. The program requires information on the connectivity and the values of the parameters characterizing beads, connectors, angles, EV potential, etc., which is supplied in a single file. An example of such an input file is shown in Figure S2 in the Supporting Information.

The hydrodynamic calculation for an array of beads is feasible using standard bead modeling procedures (for reviews, see refs 39−41). A particular difficulty in bead-model calculations has been that concerning the intrinsic viscosity, which is a key property in this work. The hydrodynamic approach of Kirkwood and Riseman,[43,44] on which bead-model methods are based, does not take into account the volume of the beads in the model, which may give rise to erroneous values of the intrinsic viscosity when the size of the beads are not much smaller than the size of the molecule modeled by them. An improved theory that considered this missing influence[45] arrived at the so-called volume correction for the intrinsic viscosity

$$[\eta](corr) = [\eta](uncorr) + f_\eta(5N_AV/2M) \quad (3)$$

where N_A is the Avogadro's number, M the molecular weight of the solute, and V the volume of the bead model. In the original

(36) Bird, R. B.; Curtiss, C. F.; Armstrong, R. C.; Hassager, O. *Dynamics of Polymeric Liquids, Kinetic Theory*, 2nd ed.; John Wiley and Sons: New York, 1987; Vol. 2.
(37) Zimm, B. H. *Macromolecules* **1980**, *13*, 592.
(38) García de la Torre, J.; Jiménez, A.; Freire, J. J. *Macromolecules* **1982**, *15*, 148.
(39) García de la Torre, J.; Freire, J. J. *Macromolecules* **1982**, *15*, 155.
(40) García de la Torre, J.; Bloomfield, V. A. *Q. Rev. Biophys.* **1981**, *14*, 81.
(41) García de la Torre, J.; Navarro, S.; López Martínez, M. C.; Díaz, F. G.; López Cascales, J. J. *Biophys. J.* **1994**, *67*, 530.
(42) Carrasco, B.; García de la Torre, J. *Biophys. J.* **1999**, *76*, 3044.
(43) Kirkwood, J. G.; Riseman, J. *J. Chem. Phys.* **1948**, *16*, 565.
(44) Kirkwood, J. G. *J. Polym. Sci.* **1954**, *12*, 1.
(45) Carrasco, B.; García de la Torre, J. *Eur. Biophys. J.* **1998**, *27*, 549.

derivation $f_\eta = 1$ so that the correction is the Einsteinian viscosity of a sphere of the same volume as the model. In some preliminary predictions of the intrinsic viscosity of dendrimers, eq 3 was applied with full volume correction.[23] More recently an application of this correction to a variety of bead models[46] showed that while $[\eta](uncorr)$, with $f_\eta = 0$, is a lower bound that always underestimates the correct value, the result with full volume correction, $[\eta](corr)$ with $f_\eta = 1$, produces an upper-bound overestimation. Clearly, an intermediate correction with $0 < f_\eta < 1$ would be more appropriate. With results gathered for such a collection of bead models, an empirical correlation has been determined between the optimum f_η and two features of the model, namely its asphericity and its degree of fragmentation. The present version of the hydrodynamic calculation routines, inserted in MONTEHYDRO, includes the determination of the optimum f_η and the corresponding volume correction. Thus, the study of the intrinsic viscosity of dendrimers does not require us to consider f_η as an adjustable parameter.

2.3. Global Properties, Equivalent Radii, and Ratios of Radii. In this work we obtain macromolecular global properties like the radius of gyration, R_g, the intrinsic viscosity, $[\eta]$, and the translational diffusion coefficient, D_t (equivalently the translational friction coefficient, f_t) of the different dendrimer structures. For the presentation and discussion of results, we shall make use of the concepts of equivalent radii and ratios of radii.[47] For a given value of a solution property, the equivalent radius is the radius of a spherical particle having the same value of that property as that of the macromolecule under consideration.[47] Equivalent radii for different properties are slightly but not greatly different and present dependences on size and shape that are more similar than the values of the properties themselves. Thus their use is particularly adequate when different properties are analyzed jointly. The equivalent radius for the translational frictional coefficient (derived from either diffusion or sedimentation coefficient) is

$$a_T = \frac{f_t}{6\pi\eta_0} \tag{4}$$

where η_0 is the solvent viscosity. It is also called the Stokes radius or hydrodynamic radius.

Another equivalent radius can be derived from another hydrodynamic property, the intrinsic viscosity, based on the Einstein formula for the intrinsic viscosity of a sphere,

$$a_I = \left(\frac{3[\eta]M}{10\pi N_A}\right)^{1/3} \tag{5}$$

where M is the polymer molecular weight and N_A the Avogadro number. In many works where intrinsic viscosity is measured,[31,48] a_I is also called the hydrodynamic radius. a_T and a_I are not identical, but studies for a great variety of structures, rigid and flexible,[47] show that their values are quite close, differing typically by less than 10%. Yet another equivalent radii is derived from the root-mean-square radius of gyration,

$$a_G = \sqrt{\frac{5}{3}}R_g \tag{6}$$

where $R_g = \sqrt{\langle s^2 \rangle}$ for a flexible structure, as in the case of dendrimers.

Ratios of any pair of equivalent radii can be formulated. We will employ the ratios $GI = a_G/a_I$, $GT = a_G/a_T$, and $IT = a_I/a_T = GI/GT$. Equivalent radii for the various properties are obviously identical for a spherical particle. For any other particle, they differ but not by very much. Thus, the ratios are unity for a spherical particle and differ from, but keep close, to unity for other conformations. The fact that $a_T \approx a_I$ so that $IT \approx 1$ (which will be particularly true for dendrimers due to their nearly spherical overall conformation) can be used as a good test for calculation procedures of the two hydrodynamic properties. GI departs more markedly from unity, but it is expected to be close to unity for a nearly spherical distribution of segments.

2.4. Distributions of Distances and Mass and Scattering Intensities. We have evaluated the distribution of distances r, between pairs of points in the dendrimer, $p(r)$, and the distribution of the radial distances $g(r)$, from the center to any point within the molecule. For this calculation, we have taken into account that the elements in our coarse-grained model are not points but spheres of finite radius a. Using expressions[49] that are presented in section 2 of the Supporting Information, these distribution functions are evaluated for each instantaneous conformation of the dendrimer, and the final result is the average over all the generated conformations. We also analyze how the mass is distributed inside the dendrimer by using a mass density distribution function, $\rho(r_C)$, where r_C is the distance from the center of the dendrimer, that is related to the radial distribution function, $g(r_C)$, through the following expression,

$$\rho(r_C) = \frac{Mg(r_C)}{N_A 4\pi r^2} \tag{7}$$

The angular dependence of the intensity of radiation scattered is represented by the scattering function (or scattering form factor), $P(h)$, where the angular variable is $h = (4\pi/\lambda)\sin(\theta/2)$, with θ as the scattering angle and λ as the radiation wavelength.[50] As the pair distribution function has been evaluated previously, $P(h)$ can be obtained directly from it:

$$P(h) = \int_0^\infty p(r)\frac{\sin(hr)}{hr}\,\mathrm{d}r \tag{8}$$

3. Atomistic Calculations

In our multiscale approach the values of all of the parameters defining the coarse-grained model of a particular dendrimer molecule, i.e., parameters for bonded and nonbonded interactions (spring and EV potentials) and bead radii, are assigned from atomistic Langevin molecular dynamics simulations of the part of the dendrimer represented by those coarse-grained elements. Therefore, the model does not have free parameters to be fit to experimental data. The molecular dynamics simulations were carried out by using the commercial software HYPERCHEM (http://www.hyper.com) with the AMBER force field at $T =$ 300 K. The simulation conditions were as follows: time step $\Delta t = 0.001$ ps, collision frequency 100 ps^{-1}, and duration of

(46) García de la Torre, J.; Del Río Echenique, G.; Ortega, A. *J. Phys. Chem. B* **2007**, *111*, 955.
(47) Ortega, A.; García de la Torre, J. *Biomacromolecules* **2007**, *8*, 2464.
(48) Tande, B. M.; Wagner, N. J.; Mackay, M. E.; Hawker, C. J.; Jeong, M. *Macromolecules* **2001**, *34*, 8580.
(49) García de la Torre, J.; Harding, S. E.; Carrasco, B. *Eur. Biophys. J.* **1999**, *28*, 119.
(50) Glatter, O.; Kratky, O. *Small Angle X-ray Scattering*; Academic: New York, 1982.

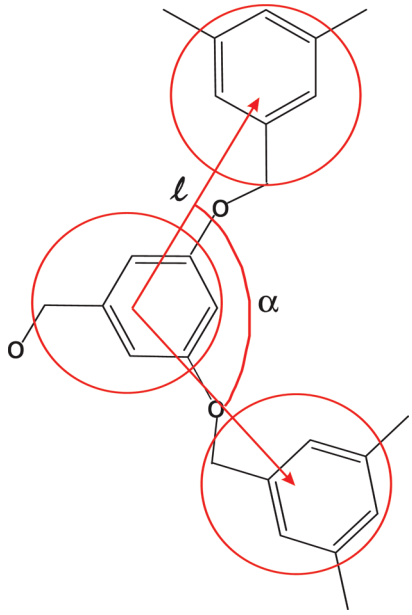

Figure 3. Atomic structure of mono-PBzE, $G = 1$, showing the beads, connectors, and angles.

the trajectory ~100 ns; under those conditions we found that simulations are well equilibrated and produce reproducible data (it was tested that other choices of the collision frequencies give nearly identical results, which are also unchanged with shorter time steps or longer trajectories; for further information see Figure S3 in the Supporting Information).

(1) Beads: The atomistic simulation with HYPERCHEM allows us to sweep the conformational space of the dendrimer monomeric unit represented by a bead. From the atomic coordinates, the Stokes radius, a_T, and the equivalent radius to radius of gyration, a_G, are computed for each conformation by using our public domain program HYDROPRO[27] (see http://leonardo.inf.um.es/macromol). Regarding the possible influence of solvation on the effective hydrodynamic radius of the atoms, we follow previous experience[52] that, in the case of small molecular entities (like the dendrimers monomeric units), such an effective radius can be equated to the van der Waals radius, of typically 1.8 Å.[51] The results are the averages over a sample of conformations. Because a_T turns out to be similar to a_G, we take as the hydrodynamic radius of the bead representing the monomer unit their mean $a = (a_G + a_T)/2$.To avoid free parameters in the model, the radius of the beads in the hard spheres EV potential was taken equal to a so that the contact distance becomes $\sigma_{HS} = 2a$. This choice seems convenient because it makes neighboring beads almost tangent and prevent "phantom" crosses of the connectors.

(2) Connector and angles: Parameters of the potentials associated to connectors and angles were estimated from atomistic simulations of the minimal atomic structure that defines those connectors and angles, as illustrated in Figure 3 for a mono-PBzE. From the atomic trajectories generated with program HYPERCHEM, the distribution functions for connector length and angle were obtained. Then we are able to set the spring potential parameters that give rise to the best fit of the Boltzmann exponential of the spring potential to those distributions obtained

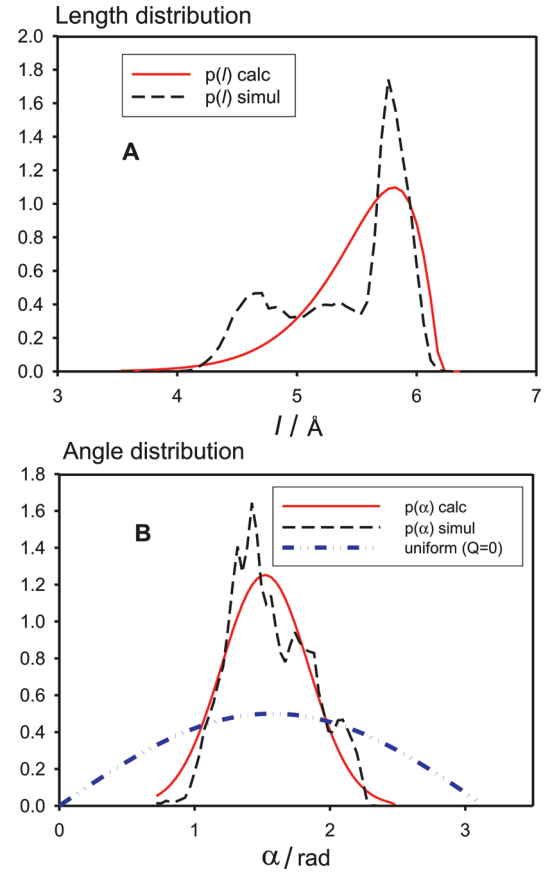

Figure 4. Distribution of lengths (A) and angles (B) in the branches of mono- and tri-PBzE. Results from the atomistic Langevin simulation and their best fits to eqs 1 and 2.

by molecular simulation. This is done by fitting the simulation results to

$$p(l) = A_l l^2 \exp[-V(l)/k_BT] \quad (9)$$

$$p(\alpha) = A_\alpha \sin\alpha \exp[-V(\alpha)/k_BT] \quad (10)$$

where A_α and A_l are normalization constants.

In that way, we obtained the values for the parameters of the coarse-grained models of the four studied dendrimers: mono-PBzE, tri-PBzE, PAMAM-EDA, and PPI-DAB (see collection of parameters in section 3 of the Supporting Information). For example, for tri-PBzE, we must distinguish between bead and springs in the core and beads and springs associated to the branches. In regard to the branches—which are the same as those in mono-PBzE—the HYDROPRO result for the equivalent radius is $a = 3.2$ Å. The atomistic simulation yields the distribution functions for the branch length and interbranch angle shown in Figure 4. Fitting $p(l)$ to the Boltzmann distribution associated to eqs 1 and 9, we get $H_{HF} = 408$ erg/cm^2, $l_{max} = 7.8$ Å, and $l_e = 5.2$ Å, and the fit of the simulated $p(\alpha)$ to eqs 2 and 10 gives $Q = 1.22 \times 10^{-13}$ erg and $\alpha_0 = 1.05$ rad. The fitted equations are compared to the simulation results in Figure 4. We remark that the fits do not reproduce the details of the simulated distribution functions—as it corresponds to a coarse-grained representation of the true potentials—but provide continuous potential functions that are conveniently handled in the Monte Carlo and dynamics simulations of the coarse grained model (indeed, we have verified that the first few moments of the fitted distribution match rather well the simulated ones).

(51) Bondi, A. *J. Phys. Chem.* **1964**, *68*, 441.
(52) Espinosa, P.; García de la Torre, J. *J. Phys. Chem.* **1987**, *91*, 3612.

Regarding the core−branch parameters, we proceed in the same way, finding $a = 4.5$ Å for the bead that represents the core, and $H_{HF} = 4040$ erg/cm^2, $l_{max} = 10.3$ Å, $l_e = 8.3$ Å, $Q = 8.28 \times 10^{-13}$ erg, and $\alpha_0 = 1.1$ rad. The sets of the parameters for the four kinds of dendrimers considered in this work are listed in section 3 of the Supporting Information.

4. Results

4.1. Conformational Distribution Functions. Figures S4−S7 in the Supporting Information show the mass density distribution functions $\rho(r)$ obtained for generations ranging from $G = 1$ to $G = 7$ for the dendrimer for the four dendrimers. The peak at very small distance corresponds to the core of the molecule, represented in the model by the central bead, but its sharpness is excessive, due to an artifact arising from the model discretization that exaggerates the high density of the core due to the almost absence of empty space.

The interesting region is that beyond the very center of the molecule, at intermediate and longer distances. At intermediate distances inside the dendrimer, the density profile shows a slight increase or tends to reach a "plateau" that is higher and broader as the generation number increases. Finally the mass density profile presents a soft decay along a range of distance of ∼10 Å where the density decreases until a value that exceeds a_G. Some examples of density profiles are depicted in Figure 5A.

These findings are in agreement with a great amount of both experimental[35,53−55] and simulation[8,13,56− 60] data that also predict a density profile more or less uniformly distributed inside the dendrimer with a decay at the dendrimer surface, which can be explained by backfolding of the end branches toward the dendrimer core. As an example of the agreement between our results and those of other workers, the density profile calculated with our coarse-grained model of PAMAM-EDA with $G = 5$ is compared to that obtained by Götze and Likos[59] in Figure 5B. These density profiles suggest a dendritic structure closer to the dense core model predicted by the Monte Carlo simulations of Lescanec and Muthukumar[7] than to the dense shell model, which was the hypothesis initially proposed by De Gennes and Hervet.[6]

A mean density of the whole dendrimer can be evaluated as the ratio of the molecular mass to the volume of the sphere with the same radius of gyration, given by $\bar{\rho} = 3M/(4\pi N_A a_G^3)$. Values are listed in Tables S5−S8 in the Supporting Information. In all cases, $\bar{\rho}$ values for dendrimers with an increasing number of generations G show an increase for the largest G's. This effect is most pronounced for PAMAM-EDA and least for mono-PBzE. This finding and the different density profiles between the molecules are explained by the greater flexibility

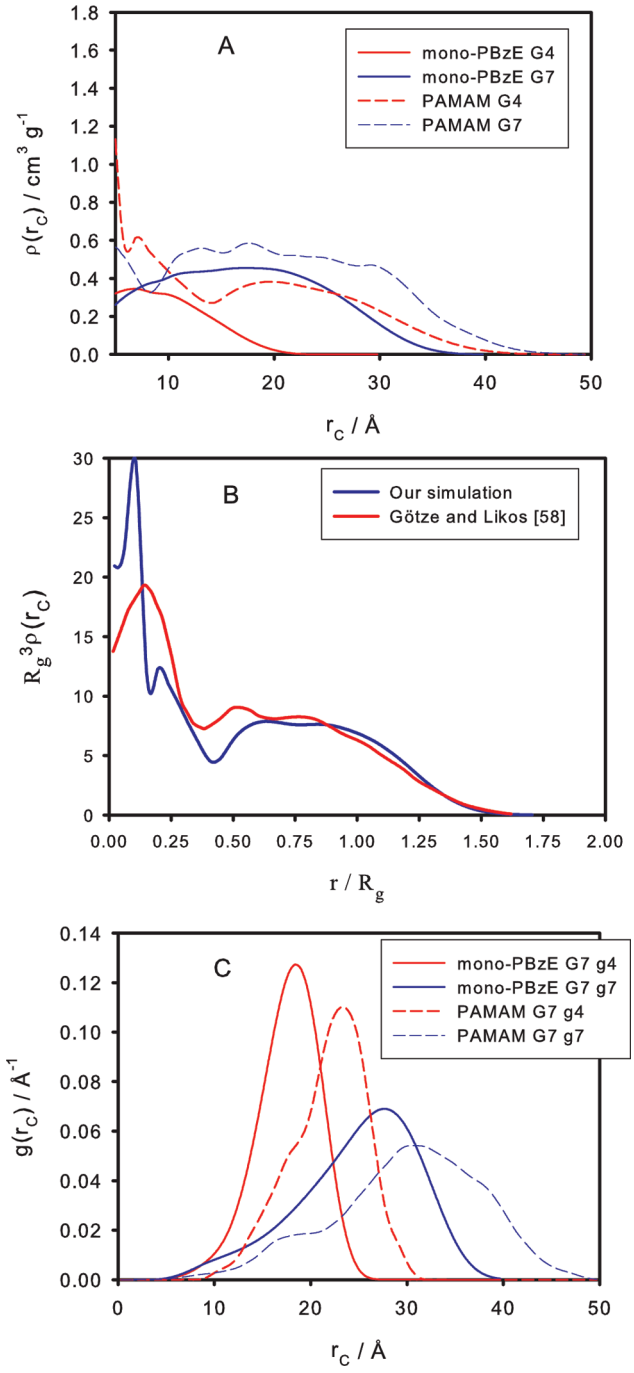

Figure 5. (A) Mass density distribution $\rho(r_C)$ within dendrimers of PAMAM-EDA and mono-PBzE with $G = 4$ and $G = 7$. (B) Comparison of our results for PAMAM-EDA of $G = 5$ with those of Götze and Likos.[59] (C) Radial distributions $g(r_C)$ for the end nodes of branches $g = 4$ and $g = 7$ of mono-PBzE and PAMAM-EDA with $G = 7$.

of the branches and nodes in PAMAM-EDA, which allows for a more intense backfolding effect. This is illustrated in Figure 5C, which shows the radial distributions of the end nodes of intermediate branches with $g = 4$ and end branches of $g = 7$, for PAMAM-EDA and mono-PBzE. The terminal branches have a higher probability to be in the interior of the molecule in the case of PAMAM-EDA.

4.2. Overall Size and Shape. The radius of gyration R_g gives a direct measurement of the mean molecular size, and the

(53) Prosa, T. J.; Bauer, B. J.; Amis, E. J.; Tomalia, D. A.; Scherrenberg, R. *J. Polym. Sci.: Part B: Polym. Phys.* **1997**, *35*, 2913.
(54) Wooley, K. L.; Klug, C. A.; Tasaki, K.; Schaefer, J. *J. Am. Chem. Soc.* **1997**, *119*, 53.
(55) Gorman, C. B.; Hager, M. W.; Parkhurst, B. L.; Smith, J. C. *Macromolecules* **1998**, *31*, 815.
(56) Maiti, P. K.; Çağin, T.; Wang, G.; Goddard, W. A., III. *Macromolecules* **2004**, *37*, 6236.
(57) Maiti, P. K.; Çağin, T.; Lin, S.-T.; Goddard, W. A., III. *Macromolecules* **2005**, *38*, 979.
(58) Harreis, H. M.; Likos, C. N.; Ballauff, M. *J. Chem. Phys.* **2003**, *118*, 1979.
(59) Götze, I. O.; Likos, C. N. *Macromolecules* **2003**, *36*, 8189.
(60) Jana, C.; Jayamurugan, G.; Ganapathy, R.; Maiti, P. K.; Jayaraman, N.; Sood, A. K. *J. Chem. Phys.* **2006**, *124*, 204719–1.

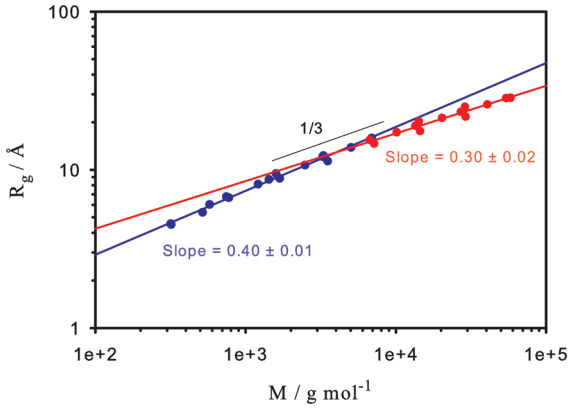

Figure 6. Radius of gyration of the four dendrimers, with generations $G = 1-7$, plotted altogether vs molecular weight, showing the two regions with different scaling exponents.

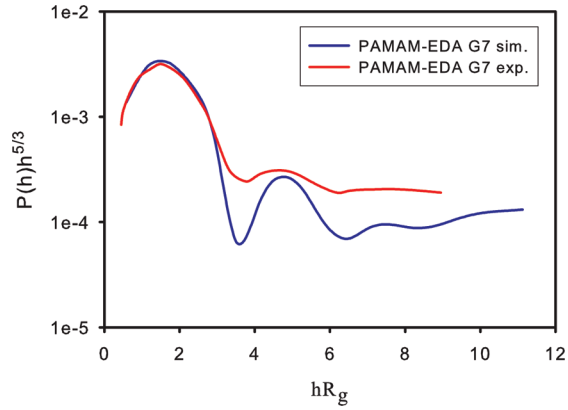

Figure 7. Kratky plot for the variation of X-ray scattering intensity for PAMAM-EDA with $G = 7$: experimental values (Prosa et al.[35]) and our simulations.

asphericity A (calculated by the method of Wei and Eichinger[24,61]) gives an idea of the anisotropy of the particle shape or mass distribution.

Figure 6 is a double-logarithmic plot that represents the variation of R_g with the molecular mass, M, for all 28 dendrimers studied in this work. It is remarkable that all the dendrimers superimpose quite well in a plot that in a first approximation could be considered a straight line of slope 0.35. But a more detailed fit shows that the curve has two slopes, 0.4 for molecular weights up to ~20 000 g/mol and 0.3 from that value up to the highest value studied here. This means that two power laws relating the radius of gyration and molecular weight are found. Some theoretical calculations and simulations[13,62] predict a slope of 0.33, and molecular dynamics simulations of Karatasos et al.[34] report a value of 0.35. However, there is some controversy about the existence of a unique power law.[59] Thus, there are also some works where authors find two regions of different slopes in the double-logarithmic plot[59,60,63] with values similar to those obtained from our fit. Indeed, the behavior observed in Figure 2 in ref 62 showing experimental values of R_g vs M for several dendrimers is similar to that displayed in our Figure 6 with a change in the slope for a molecular weight of 20 000 g/mol.

A value of the slope (exponent of the power law) of $^1/_3$ is the expectation for spherical particles (of uniform density), and it is consistent with some structural studies on dendrimers.[64] Also, it is worth mentioning that simulations of Sheng et al.[65] show that, for an increase in M associated to an increase in the number of generations, the exponent is closer to $^1/_3$, but if it is due to an increase in the branch length and mass, the exponent should be close to $^1/_5$ as found by Lescanec and Muthukumar.[7] Another reason for the change in exponents is that for low M and G the dendrimers are semiflexible and appreciably nonspherical, as revealed by the high values of the asphericity, so that the exponent should be larger than $^1/_3$. On the other hand, for high G, the mass distribution of the dendrimers is practically spherical, as revealed by the very low values of the asphericity (Tables S5−S8 in the Supporting Information). However the increase in R_g with M is smaller than it should be for spheres of constant density because of, again, the backfolding effect: external branches have some tendency to get back to the core, and therefore the effective volume, proportional to R_g^3, grows slower than M and the exponent of R_g vs M is below $^1/_3$.

4.3. X-ray Scattering. The angular variation of intensity in small-angle X-ray scattering (SAXS), represented by the (normalized) form factor, $P(h)$, provides very valuable information not only about the overall size and shape but also about the internal structure. Beyond the region of very low h, which is determined simply by the radius of gyration, at higher h's scattering intensities are strongly influenced by the distribution of mass within the dendrimer. For the four dendrimers, up to $G = 7$, we have evaluated the $P(h)$ functions, which are presented in Figures S4−S7. Scattering intensities are usually presented in the form of Kratky plot $P(h)(hR_G)^{5/3}$ vs hR_g. For PAMAM-EDA, experimental plots of dendrimers up to $G = 10$ were reported by Prosa et al.[35] and are compared in Figure S8 with our simulation results. The similarity of experimental and simulated diagrams is striking. The agreement is not only qualitative. In Figure 7 we compare in the same graph our simulation result for a PAMAM-EDA of $G = 7$ with that coming from SAXS experiments by Prosa et al.[35] (as their intensities are in arbitrary units, we have renormalized with a constant so that the positions of the primary peak are matched). Clearly, there is a good agreement between experiment and simulation over the whole angular range. The two relevant peaks, the valleys, and the end "plateau" are reproduced by the simulations at the same positions, i.e., at the same values of the scattering angles. The fact that simulation results give rise to deeper valleys can be due to the discretization of the model. Valleys deeper than those in experimental results are also obtained in other computational works.[66]

Unfortunately, the only systematic data of scattering intensities that reflect so well the overall and internal structure of dendrimers are those by Prosa et al.[35] Similar results for other dendrimers are, to the best of our knowledge, still unavailable.

5. Hydrodynamic Properties and Equivalent Radii

As indicated above, from our simulations we have also predicted—in a multiscale approach, without adjustable parameters—overall solution properties for which some experimental data are available.

(61) Wei, G.; Eichinger, B. E. *J. Chem. Phys.* **1990**, *93*, 1430.
(62) Boris, D.; Rubinstein, M. *Macromolecules* **1996**, *29*, 7251.
(63) Mallamace, F.; Canetta, E.; Lombardo, D.; Mazzaglia, A.; Romeo, A.; Mons Scolaro, L.; Maino, G. *Physica A* **2002**, *304*, 235.
(64) Pötschke, D.; Ballauff, M.; Lindner, P.; Fischer, M.; Vögtle, F. *Macromolecules* **1999**, *32*, 4079.
(65) Sheng, Y. J.; Jiang, S.; Tsao, H.-K. *Macromolecules* **2002**, *35*, 7865.
(66) Rathgeber, S.; Pakula, T.; Urban, V. *J. Chem. Phys.* **2004**, *121*, 3840.

The most frequently reported property is the intrinsic viscosity, $[\eta]$. In general, in our simulations (Figure S9) as well as in many other experimental and computational studies,[17,21,31,32] it is found that $[\eta]$ does not increase monotonically with molecular weight, unlike the case with common polymers. Instead, $[\eta]$ reaches a maximum value and then it keeps constant or even decreases. As indicated above, for high G the effective (hydrodynamic) volume of the molecule does grow with G, although that growth may be less than that of the molecular mass. Considering dendrimers as spheres, for which $[\eta]$ is related to specific volume (i.e., the ratio of volume to mass), its value would remain constant if the density does not change on going from G to $G + 1$, and it could even decrease when volume grows less than mass due to the backfolding effect. The effect is particularly visible in our simulations for the dendrimers with more flexible branches, PAMAM-EDA and PPI-DAB, that present a more marked backfolding phenomenon.

Nonetheless, the geometric or hydrodynamic size of the dendrimer grows with G. That should be reflected by the hydrodynamic radius that one would obtain from the diffusion coefficient, D. Unfortunately, measurements of this property are quite rare so far; hopefully the modern dynamic light scattering instrumentation which could allow precise measurements for such small macromolecules will soon provide such information. More abundant are the experimental results for the radius of gyration, R_g, determined from scattering intensities at very low angles. As discussed above, to make a more systematic, simultaneous treatment of the various overall properties, we have chosen to express them in the form of the equivalent radii a_G, a_T, and a_I. The results are reported in Tables S5−S8. These predictions are intended to be compared with experimental data, for which we have taken:

(1) For mono-PBzE, R_g in THF,[48] and $[\eta]$ in THF.[31]
(2) For tri-PBzE, R_g (no experimental data), and $[\eta]$ in THF.[31]
(3) For PAMAM-EDA, R_g in 0.1 M citric acid in water,[32] and $[\eta]$ in 0.1 M citric acid in water, Figure 14.2 in ref 4.
(4) For PPI-DAB, R_g in $\mathbf{D}_2\mathrm{O}$,[67] and $[\eta]$ in $\mathbf{D}_2\mathrm{O}$.[67]

We chose experimental data in solvents for which exist measurements of both R_g and $[\eta]$ to be able to compare properly their respective equivalent radii. It is remarkable that those experimental data are reproduced quite well by our simulations, especially taking into account that we do not use adjustable parameters to model solvent quality.

Figure 8 shows the equivalent radii a_G and a_I (the other hydrodynamic radius, a_T, is generally quite close to a_I) for mono-PBzE. For the other three dendrimers, similar plots are in Figure S11. At first sight, the agreement is very satisfactory. Nonetheless, we have quantified the concordance between experimental and calculated radii, in terms of a typical error, defined as the root-mean-square percent deviations:

$$\%\ diff = 100\left[\sum\left(\frac{a_X(calc) - a_X(expt)}{a_X(expt)}\right)^2\right]^{1/2} \qquad (11)$$

For a given property, X, the sum can be run over the various G's of a dendrimer and even over all the four dendrimers and over the various properties of a dendrimer or the whole set. As seen in Table 1, the typical errors for the various dendrimers of both the geometric radii a_G and the hydrodynamic radii a_T or a_I are, in most cases, of only a few percent, of the same order as the typical error of the experimental values. For a set of 26 equivalent radii, the typical deviation of our simulations from experimental data is ∼4%.

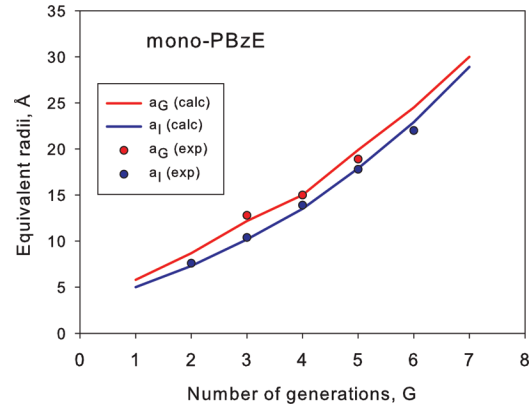

Figure 8. Equivalent radii a_G and a_I for mono-PBzE: our simulation results along with experimental values.[31,48]

Table 1. Typical Errors of the Equivalent Radii of the Various Dendrimers and Global Typical Errors

equivalent radius	dendrimer molecule	rms % diff	num. of data
a_G	mono-PBzE	7.7	3
a_I	mono-PBzE	2.9	5
a_I	tri-PBzE	6.3	7
a_G	PAMAM-EDA	3.2	3
a_I	PAMAM-EDA	2.9	4
a_T	PAMAM-EDA	5.7	3
a_G	PPI-DAB	4.1	4
a_I	PPI-DAB	2.9	4
all	mono-PBzE	5.2	8
all	tri-PBzE	6.3	5
all	PAMAM-EDA	4.0	10
all	PPI-DAB	3.2	8
a_G	all	5.3	10
a_I	all	2.9	13
a_T	all	5.7	3
a_I,a_T	all	3.6	16
all	all	4.3	26

6. Concluding Remarks

In this work we have implemented a scheme for the prediction of properties of dendrimer molecules using a very simple coarse-grained model whose parameters are not adjusted to fit experimental data, but instead they are obtained, in a multiscale approach, from previous atomistic simulations, which are also done in a simple fashion, with Langevin dynamics, not of the whole molecule, but of small pieces of it. Although the procedure has two stages and lacks adjustable parameters, it predicts geometric and hydrodynamic radii of the four dendrimers studied that agree with experimental data with a typical error of ∼4%. Furthermore, the internal distribution of mass seems to be predicted correctly, as probed by the agreement with some X-ray scattering data and other computer simulations.

The present scheme opens the possibility of studying other related systems, like functionalized or variegated dendrimers, randomly hyperbranched molecules, etc. In the present work, the adequately parametrized coarse-grained model has been simulated by a Monte Carlo procedure to obtain conformational and overall properties of the molecule, but we anticipate that the same model (with the forces derived from the analytical potentials on which it is based) could be used for Brownian dynamics simulations of the internal dynamics of the dendrimers

(67) Scherrenberg, R.; Coussens, B.; van Vliet, P.; Edouard, G.; Brackman, J.; de Brabander, E.; Mortensen, K. *Macromolecules* **1998**, *31*, 456.

in solution, to study dynamic aspects that would be out of reach of fully atomistic molecular dynamics simulations.

Acknowledgment. This work was supported by Grants CTQ-2006-06831 to J.G.T. and CTQ-2006-06446 to J.J.F. from *Ministerio de Ciencia e Innovación* and Grant 04531/GERM/06 (*Grupos de Excelencia de la Región de Murcia*) from *Fundación Séneca* to J.G.T.

Supporting Information Available: Further details on the methodology, Tables S1 to S8, and Figures S1 to S11. This material is available free of charge via the Internet at http://pubs.acs.org.

JA901275D